Studies in Engineering and Exact Sciences
ISSN: 2764-0981

Filaments of ABS loaded with Neomycin – a supplier to produce surfaces by 3D printing

Filamentos de ABS carregados com Neomicina - um fornecedor para produzir superfícies por impressão 3D

DOI: 10.54021/sesv3n3-002

Recebimento dos originais: 05/05/2022
Aceitação para publicação: 01/07/2022

Yasmin dos Anjos Garcia
Engenheira Química
Institution: Universidade Federal Rural do Rio de Janeiro
Address: Seropédica, RJ, Brazil, Km 07,Zona Rural, BR-465, Seropédica - RJ, CEP: 23890-000
E-mail: yasminanjosgarcia@hotmail.com

Hellen Regina Oliveira de Almeida
Mestre em Engenharia Química
Address: Seropédica, RJ, Brazil, Km 07,Zona Rural, BR-465, Seropédica - RJ, CEP: 23890-000
E-mail: hellenregina.oliveira@gmail.com

Luciara da Silva
Engenheira de Materiais
Institution: Universidade Federal Rural do Rio de Janeiro
Address: Seropédica, RJ, Brazil, Km 07,Zona Rural, BR-465, Seropédica - RJ, CEP: 23890-000
E-mail: luciaraufrrj@hotmail.com

Talita Goulart da Silva
Mestre em Engenharia Química
Institution: Universidade Federal Rural do Rio de Janeiro
Address: Seropédica, RJ, Brazil, Km 07,Zona Rural, BR-465, Seropédica - RJ, CEP: 23890-000
E-mail: tgoulart11@gmail.com

Débora Baptista Pereira
Mestre em Engenharia Química
Institution: Universidade Federal Rural do Rio de Janeiro
Address: Seropédica, RJ, Brazil, Km 07,Zona Rural, BR-465, Seropédica - RJ, CEP: 23890-000
E-mail: debora.d94@hotmail.com

Roberta Helena Mendonça
DoutoraCiências e Engenharia de Materiais
Institution: Universidade Federal Rural do Rio de Janeiro
Address: Seropédica, RJ, Brazil, Km 07,Zona Rural, BR-465, Seropédica - RJ, CEP: 23890-000
E-mail: robertahmendonca@ufrrj.br

ABSTRACT
The skin of several animals can be affected by bacterial infection, especially in the case of dogs and cats. Among the bacteria that can cause skin and soft tissue infections, Staphylococcus aureus (S. aureus) is one of the commonest. Neomycin (NEO) is one of the most used antibiotics to prevent bacterial infections. Due to this cochleotoxicity and nephrotoxicity, their use is topical. Animals infected by these bacteria can potentially contaminate healthy animals and humans. A possible alternative may be the development of surfaces with bactericidal properties where animals, during the treatment phase, can rest without favoring the local proliferation of the bacteria. This work aims to produce, by hot extrusion, filaments of acrylonitrile butadiene styrene (ABS) with neomycin. ABS is a thermoplastic polymer commonly used in fused deposition modeling (FDM). A mixture of ABS and NEO (1:6% w/w) was extruded, resulting in ABS/neomycin filament with a diameter of 2.4 mm. Scanning electron microscopy (SEM), X-ray diffraction (XRD), and Fourier transform infrared spectrometry (FTIR) showed that the filament might be used for the production of surfaces by 3D printing.

Keywords: neomycin, acrylonitrile butadiene styrene, hot extrusion method, filaments, bactericidal surfaces.

RESUMO
A pele de vários animais pode ser afetada por infecções bacterianas, especialmente no caso de cães e gatos. Entre as bactérias que podem causar infecções de pele e tecidos moles, o Staphylococcus aureus (S. aureus) é uma das mais comuns. A neomicina (NEO) é um dos antibióticos mais utilizados para prevenir infecções bacterianas. Devido a esta cochleotoxicidade e nefrotoxicidade, sua utilização é tópica. Os animais infectados por estas bactérias podem potencialmente contaminar animais saudáveis e humanos. Uma alternativa possível pode ser o desenvolvimento de superfícies com propriedades bactericidas onde os animais, durante a fase de tratamento, podem descansar sem favorecer a proliferação local da bactéria. Este trabalho visa produzir, por extrusão a quente, filamentos de acrilonitrilo butadieno estireno (ABS) com neomicina. O ABS é um polímero termoplástico comumente usado em modelagem de deposição fundida (FDM). Uma mistura de ABS e NEO (1:6% p/p) foi extrudida, resultando em filamento de ABS/neomicina com um diâmetro de 2,4 mm. A microscopia eletrônica de varredura (SEM), difração de raios X (XRD) e espectrometria de infravermelho por transformação de Fourier (FTIR) mostraram que o filamento pode ser usado para a produção de superfícies por impressão 3D.

Palavras-chave: neomicina, acrilonitrilo butadieno estireno, método de extrusão a quente, filamentos, superfícies bactericidas.

1 INTRODUCTION

Bacterial infections are complex and involve several aspects. Both animals and humans are prone to this type of infection. Among the different types of known pathogens capable of causing an infection, Staphylococcus aureus, a pathogen found naturally in the microbiota of the skin and some mucous membranes, causes one of the most acute infections reported in domestic animals. (MURRAY *et al*., 2017; QUINN *et al*., 2005; MCVEY, 2013). Staphylococcus aureus presents several strains resistant to the most varied classes of antibiotics, such as beta-lactams, streptomycin, aminoglycosides, chloramphenicol, sulfonamides, rifampicin, fusidic acid, and quinolones. (NARCISO et al, 2011; TALÉNS-VISCONTI; GARRIGUES; CANTÓN, 2002).

Staphylococcus delphinium and Staphylococcus pseudointermedius may cause pathogenicity in animals, including domestic animals such as dogs and cats. Staphylococcus pseudointermedius affect more canine species in different pathologies, such as pyoderma and ulcers. (MAGLEBY et al., 2019; DEVRIESE, et al. 2009; DE KNEGT, 2018). (OLIVEIRA *et al,* 2006; BOELTER *et al*, 1978; MELO *et al*, 2021). One of the problems is that animals can become contaminated through contact with the surface. Thus, developing materials to obtain bactericidal surfaces for animals undergoing treatment may be an alternative to reduce the risk of contamination.

The use of polymers in many industries, including pharmaceuticals, is common. The release properties' capability and processability turn these materials versatility. It is possible to obtain this final product containing the polymer and drugs through the hot extrusion method, from which the mixture of both is processed to obtain an extrudate with properties related to constituent's materials (SPINOSA, 2017; EL-SAY; EL SAWY, 2017; SAKS; GARDNER, 1997; RESTANI *et al*., 2010).

Acrylonitrile butadiene styrene (ABS) is a type of copolymer produced from styrene-butadiene polymers that is applied, among other things, for the production of different products due to its characteristics, among which we can mention its processability, dimensional stability, rigidity, heat, chemical and impact resistance (SIMIELLI., 1993; HIRAYAMA, 2015; ALMEIDA, 2016). In addition, ABS is a polymer widely used in 3D printing, a technique that makes it possible to obtain

different objects according to need.

This work aimed to produce 3D suppliers in the form of filaments of ABS/NEO to produce surfaces, such as blankets, to protect areas for pets in treatment infected by Staphylococcus.

2 MATERIALS AND METHODS

Figure 1. Raw materials used in the experiment (a) ABS; (b) NEO

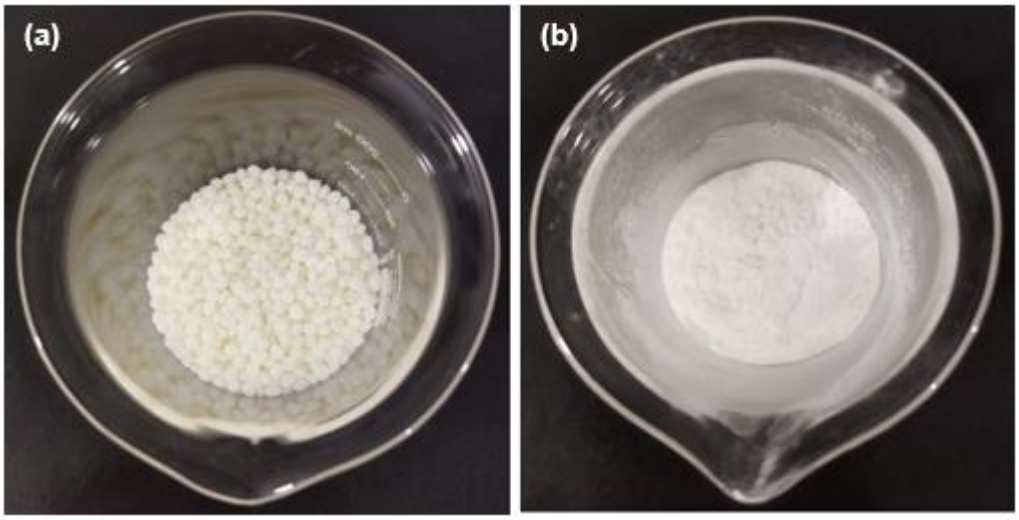

Source: Author, 2022.

2.1 PRODUCTION OF ABS/NEO FILAMENTS

The filaments were produced using an FILMAQ 3D STD extruder, Brazil. 50g of ABS and NEO were fed to the extruder at 200 ºC. The filament diameter was 1,75mm.

Figure 2. Schematic representation of the ABS/NEO filament manufacturing by extrusion.

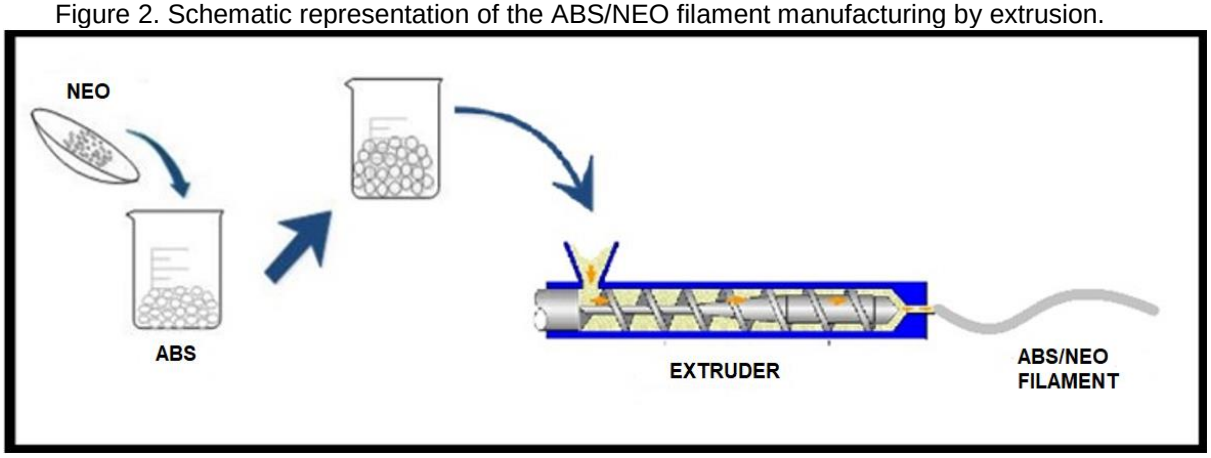

2.2 SCANNING ELECTRON MICROSCOPY (SEM)

The morphology of ABS and ABS/NEO films was evaluated using a scanning electron microscope (HITACHI model TM3000) at an acceleration voltage of 15 kV. The ImageJ® image processing program was used to highlight the segmented pores on the surfaces and measure the average size of each pore (µm) in its respective image scale.

For the morphological study, the samples were divided into three groups: surface – ABS, surface – ABS - Cut, surface ABS/NEO, and surface ABS/NEO – Cut. The division of these groups focused on analyzing by parts the morphology of pure ABS and ABS/NEO filaments. The magnitudes used were 50x, 150x, and 500x.

2.3 X-RAY DIFFRACTOMETRY (XRD)

XRD analysis of PCL, NEO, and ABS/NEO filaments was performed on an X-ray diffractometer (Rigaku, Mini Flex II model) operated with the Cukα source (λ = 1.5418 Å). The scans were recorded over the range of 2θ = 6–60°, with a scan speed of 2°. s^{-1}.

2.4 FOURIER-TRANSFORM INFRARED SPECTROSCOPY (FTIR)

A chemical analysis of the produced ABS, NEO, and ABS/NEO filaments were carried out to investigate possible interactions between ABS and NEO in the samples using an Infrared Spectrometer (Bruker, model Vertex 7) with attenuated total reflectance (ATR) by recording measurements from 4000 to 400 cm^{-1}.

3 RESULTS AND DISCUSSION

Figure 3 shows the filaments of ABS/NEO obtained by hot melting extrusion. The filament diameter was 2.4 mm, corresponding to an expansion of 50% concerning the nominal of the extrusion nozzle (1.75 mm). This result can be associated with the different thermal behavior of the polymer and drug materials.

Figure 3. (a) ABS/NEO filament and (b) ABS/NEO filament cut obtained by the hot extrusion technique.

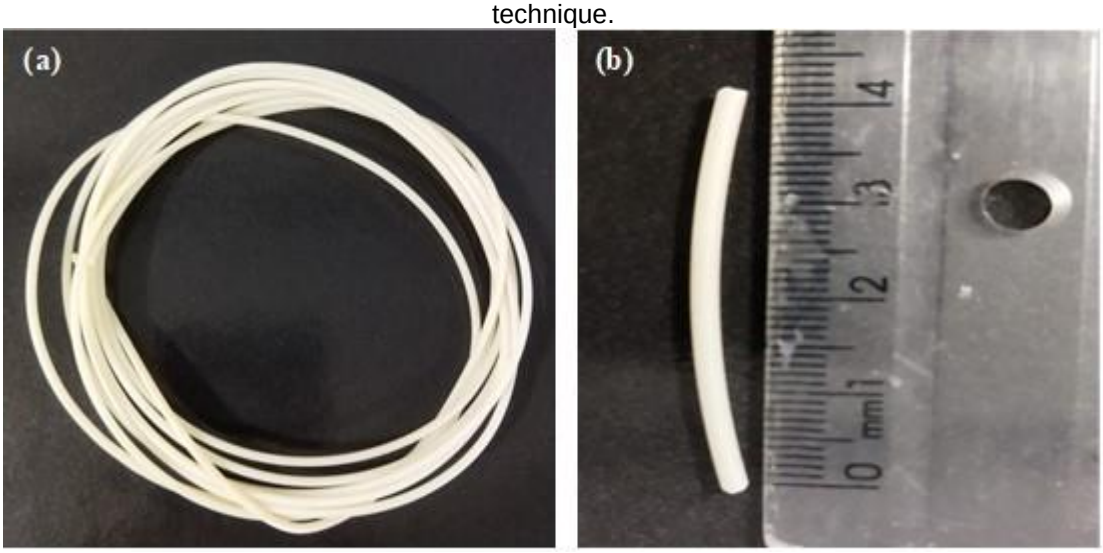

According to Alhijjaj et al. (2016), adding a drug to the ABS polymer promotes changes in rheological behavior. In the present work, the filament cooled to room temperature in contact with air. One possibility to reduce the diameter expansion is reducing the cooling temperature, thus offering less time for the expansion. For 3D printing, the material must have a low melting viscosity at the printing temperature.

3.1 FOURIER-TRANSFORM INFRARED SPECTOMETRY (FTIR) ON ABS/NEO FILAMENTS

Figure 4 shows the FTIR spectra of the ABS and NEO materials themselves and the ABS/NEO filament. The ABS and NEO bands were summarized in Tables 1 and 2, respectively.

Figure 4. FTIR spectres of ABS, NEO and the ABS/NEO filament. The highlighted rectangles I, II and III denotes some of the characteristic bands of the raw materials in order to help the results interpretation.

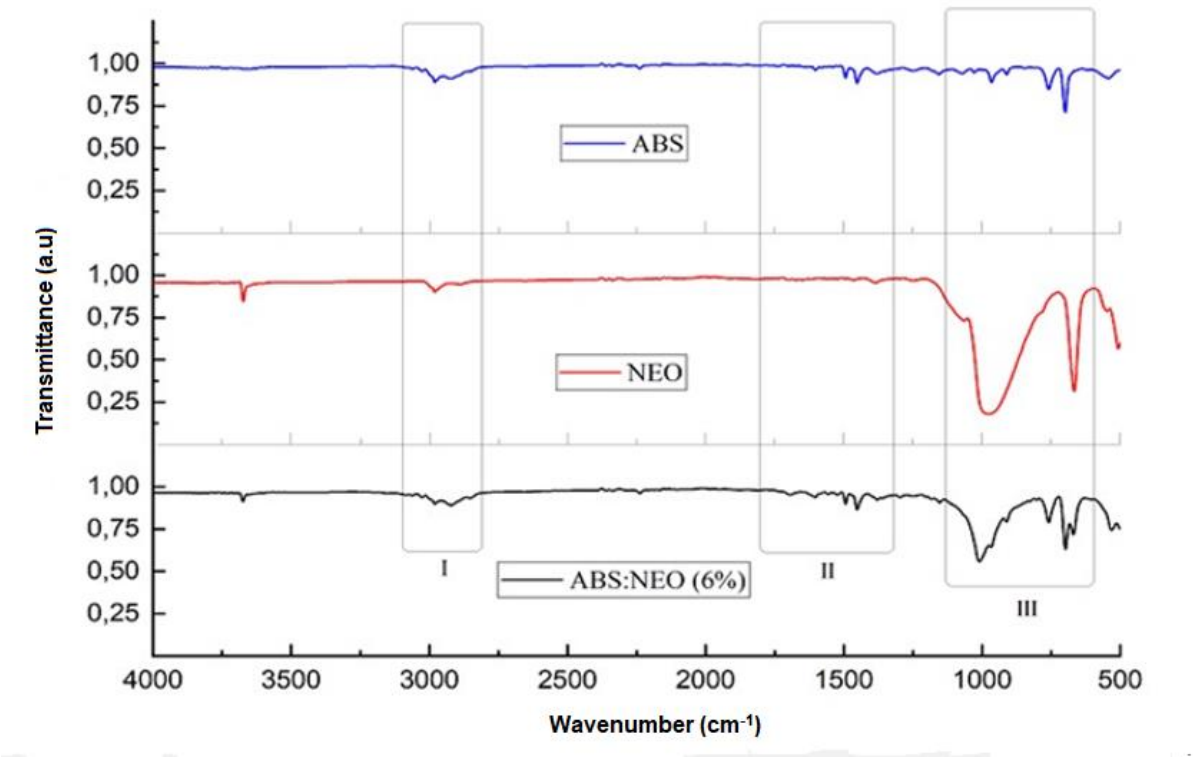

The characteristic bands of ABS are in agreement with the literature, as shown in Table 1. In this work characteristic bands of NEO differ a little from those reported in the literature, as observed in the region between 3550 and 3200 cm^{-1}, where the value obtained for NEO was 3673 cm^{-1}, and between 1260 and 1000 cm^{-1}, where the band obtained was 977 cm^{-1} (REBITSKI et al., 2018; SWATHIL et al., 2013; CANDIDO, 2019).

Table 2 shows characteristic bands of NEO. Some NEO bands occur in the same region as the bands associated with ABS, thus, overlapping of these bands may occur, as shown in Figure 4 and highlighted in I, II, and III. It is worth mentioning that the proportion of the components in mixtures can affect the intensity of the bands. ABS/NEO filaments present bands related to NEO and ABS. No new bands appear in the ABS/NEO spectrum. All bands are related to the pure components, which indicates that there was no formation of chemical bonds, which is an advantage because there was no chemical change in the drug.

Table 1. Correlation between wave length (cm^{-1}) of infrared absorption for ABS.

Wave length (cm^{-1}) (Literature)	Wave length (cm^{-1})	Attribution
3085 - 2920	2979	C−H (axis deformation)
2250 - 2239	2237	C≡N
1452	1452	CH_2
965-910	966	C−H
760-758	759	=C−H
702 - 698	698	C−H (bond angular deformation in the aromatic ring)

Source: LUNA *et al.*, 2020; NEHER *et al.*, 2014.

Table 2. Correlation between wave length (cm^{-1}) of infrared absorption and chemical structure of NEO.

Wave length (cm^{-1}) (Literature)	Wave length (cm^{-1})	Attribution
3550 - 3200	3673	O-H
2890 -3100	2979	C−H
1260 - 1000	977	C−O
815 - 602	677	N−H (out of plane bending)

Source: REBITSKI *et al.*, 2018; SWATHIL *et al.*, 2013; CANDIDO, 2019.

3.2 X-RAY DIFFRACTOMETRY (XRD) ON RAW MATERIALS AND ABS/NEO FILAMENTS

Figure 5 shows the X-ray diffractogram of ABS, NEO, and ABS/NEO filament, with the abscissa axis between 0 and 45 (2θ).

Figure 5. X-Ray Diffractogram of ABS, NEO, and ABS/NEO filament between 0 and 45 (2θ)

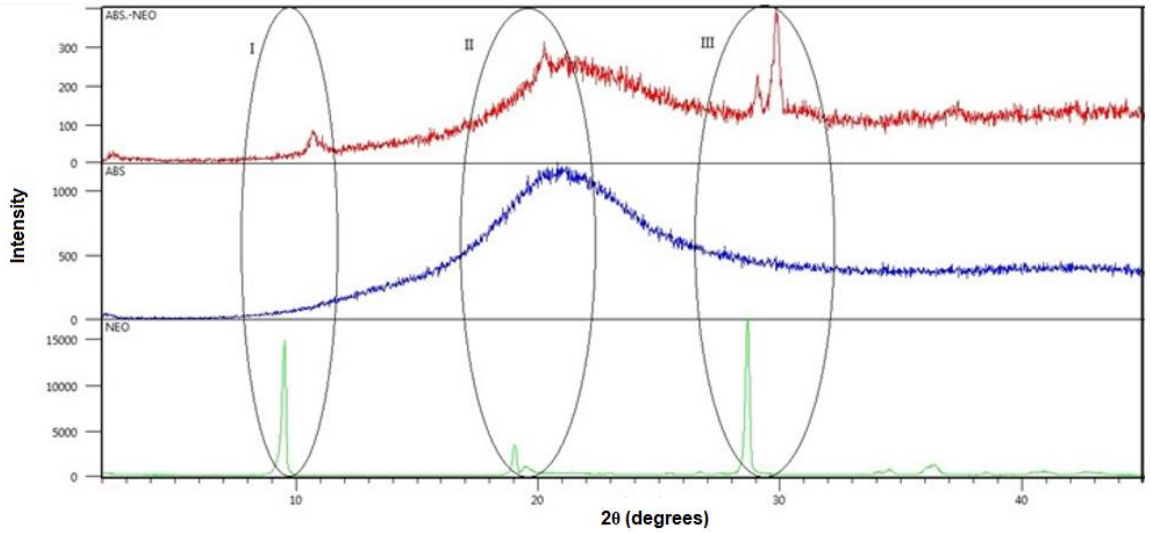

The circled regions in I, II, and III (Figure 5) indicate some of the characteristic bands of the pure materials. For NEO, in the X-ray diffractogram (Figure 5), the peaks observed are: 2θ equal to 9.51°; 19.1°; 19.5°; 28.7°; 36.5°. According to the literature, the characteristic peaks of NEO are at approximately 2θ, equal to 9.1°; 19.46°; 23.64°; 36.1° (SCHEIDT, 2018; CANDIDO, 2019). ABS, according to the diffractogram, is an amorphous polymer. Peaks were observed at approximately 2θ, equal to 1º to 4.8º, which agrees with the literature (AALAIE, RAHMATPOUR, 2007; NEHER et al., 2014). The prominent peaks observed for the polymer, represented in II (2θ = 19.8º and 20.9º), also agree with the literature. (NEHER et al., 2014; SHISHAVAN; AZDAST; AHMADI, 2014). The ABS/NEO filament has peaked at approximately 2θ equal to 10.5°; 19.8°; 28.8°, and 29.5°. Compared to the NEO diffractogram, the ABS/NEO filaments show the characteristic peaks of the drug, as shown in I, II, and III. In addition, it is possible to observe that there were no significant changes in pick position compared to the pure materials. That is, both the drug and polymer characteristics.

3.3 MORPHOLOGICAL ANALYSIS - SCANNING ELECTRON MICROSCOPY (SEM)

Figure 6 shows the surface and fracture surface of pure ABS. The surface of the pure polymer filament has uniformity and few unfilled spaces, indicating a good extrusion process. According to Neher *et al.* (2014), the unfilled spaces occur

due to the low adhesion of the polymer to the hot extrusion process.

Figure 7 shows the micrographs of the ABS/NEO filament. The ABS/NEO filament presents an irregular surface due to the presence of NEO. In the zoom images in (a), (b) and (c) it is noted that the cut surface of the ABS/NEO filament is porous. According to Mir *et al*. (2017), the size of the pores present in the polymer-drug filament favors the drug release kinetics, as long as the drug particle size is compatible with the pore dimensions (MIR; ANSARI; ALI, 2017).

In order to better explore the scanning electron microscopy data, ImageJ image processing software was used to highlight the segmented pores in the images and define the average size of each pore (µm) in the respective magnitude. The area marked in red corresponds to the surface and the darkened area is representing the pores (by depth). According to the porosity mapping shown in Figure 8, image (a), which represents the photomicrograph of the average cut surface of the ABS filament with a magnitude of 500x, 113 pores with a size of 3,242 µm were found. Image (b) represents the micrograph of the cut surface of the ABS/NEO filament with a magnitude of 500x, where the software has mapped 54 pores with an average size of 12,074 µm.

It is possible to see (Figure 8 b) white particles relative to the NEO. Candido (2019) also observed NEO particles similar to the present work. Candido (2019) studied the interaction of the drug NEO with alginate microparticles. In the study by Singh & Jonnalagadda (2021), these particles also appear in which were produced, through 3D printing, using the poly(lactic acid) polymer loaded with neomycin.

Based on SEM, XRD, and FTIR the ABS/NEO filaments are adequate for 3D printing because the drug was well distributed on the polymer matrix.

Figure 6. Scanning electron microscopy photomicrographs of the surface and fracture surface of the ABS filament.

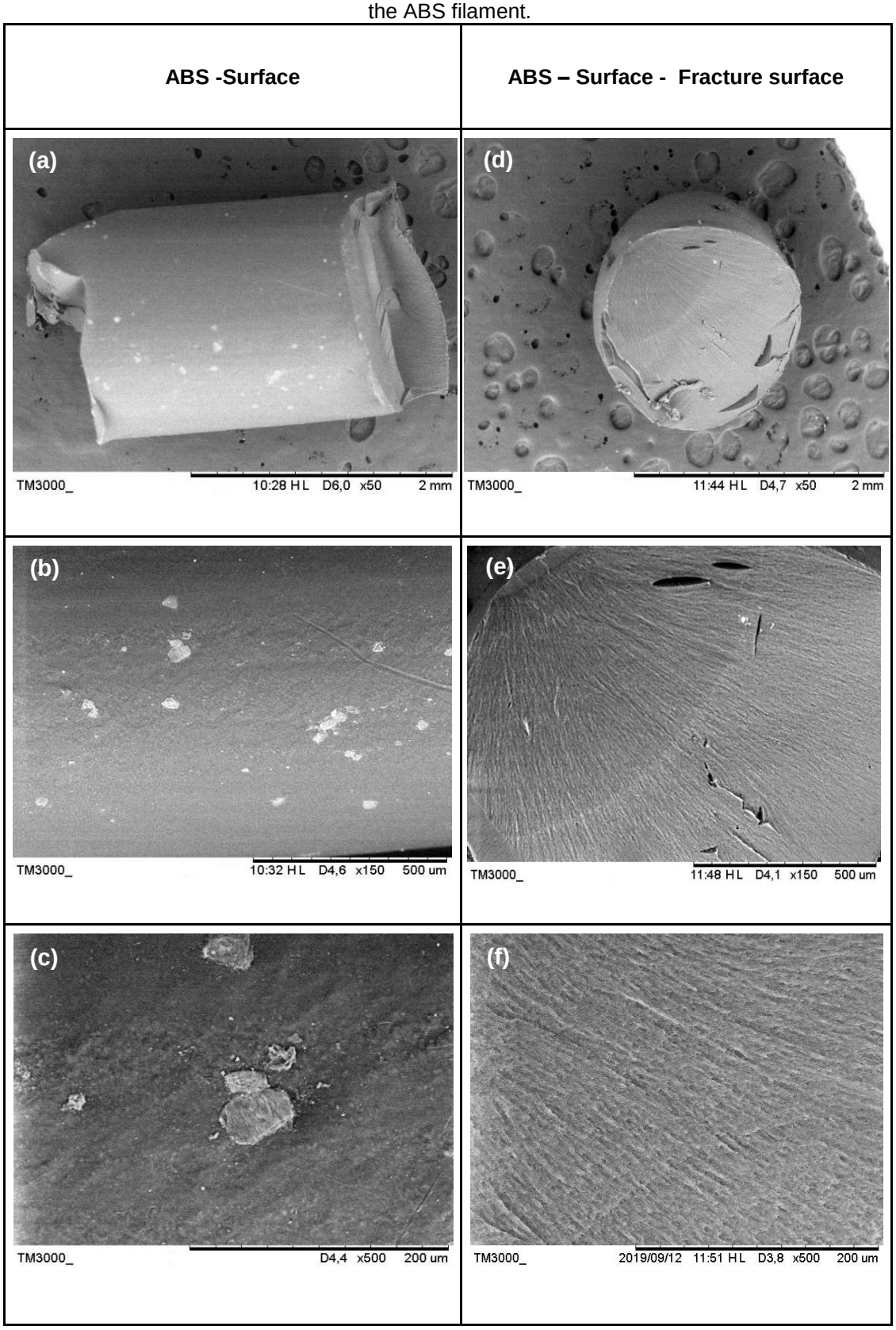

Figure 7. Scanning electron microscopy (SEM) photomicrographs of the surface – fracture surface of the ABS/NEO filament

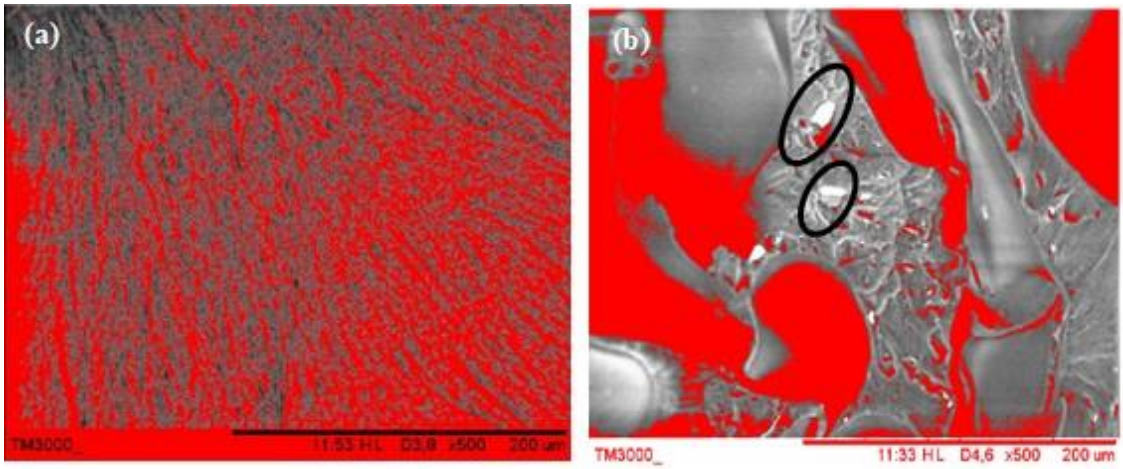

Figure 8. Photomicrographs with porosity mapping of (a) the cut surface of the ABS filament and (b) the cut surface of the ABS/NEO filament

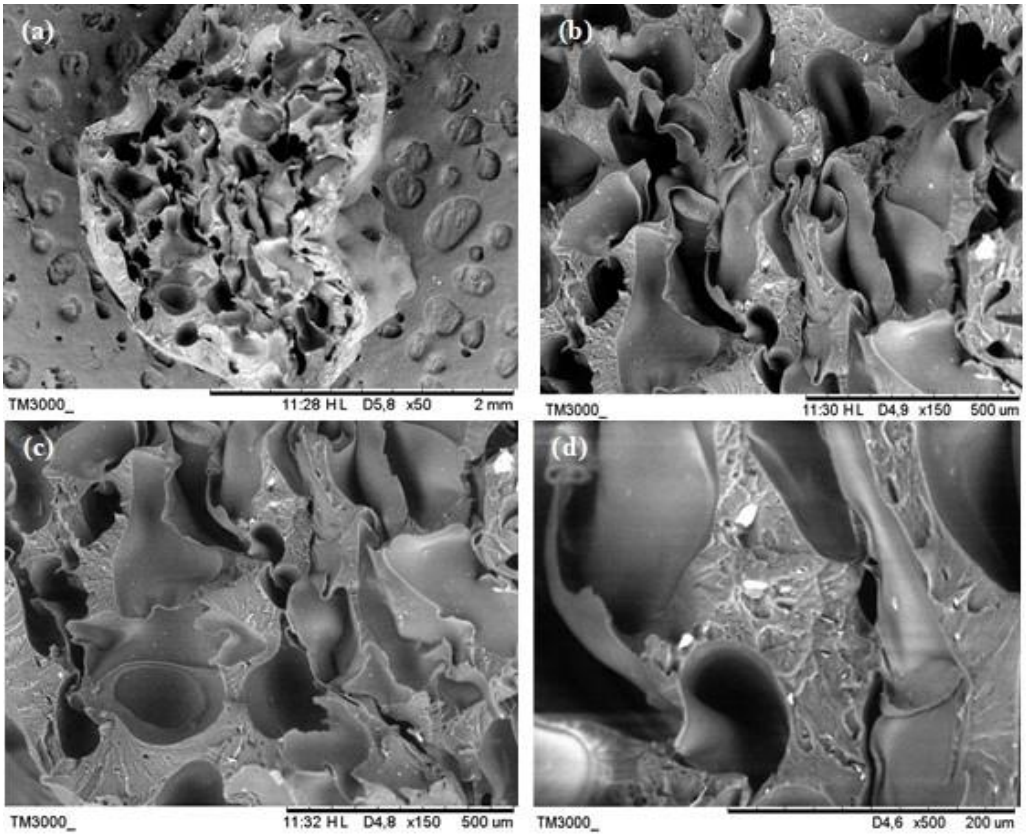

4 CONCLUSION

In the present work, the ABS filaments containing the drug NEO were successfully obtained, that is, as expected, and the characterizations performed FTIR, DRX and SEM were adequate for preliminary studies, which represents a good indication for the development of bactericidal surfaces through 3D printing.

The images obtained by SEM showed non-uniformity in the ABS/NEO filaments, however, as mentioned in the literature, this is not a problem, since the pores present in the filament corroborate the release of the drug. For further conclusions on this statement, it is necessary that thermal analyzes are carried out with the ABS/NEO filaments.

The XRD technique used in the present work proved to be effective since the characteristic peaks of the drug and the polymer were observed in all the studied samples and it was showed that, in the ABS/NEO filaments, the characteristics of the drug were preserved.

For the FTIR analysis, the corresponding bands of both the drug and the polymer in the produced filament were observed. In addition, no displacement of the ABS and NEO bands was observed in the filament, which characterizes that there was no formation of strong intermolecular interactions between the ABS/NEO filament. The non-emergence of new bands proves that there was no reaction.

Therefore, according to the data obtained, it is possible to suggest that the filament produced from ABS polymer loaded with NEO is a good model for initial studies for the development of bactericidal surfaces.

REFERENCES

AALAIE, Jamal; RAHMATPOUR, A. Study on Preparation and Properties of Acrylonitrile-Butadiene-Styrene/Montmorillonite Nanocomposites. **Journal of Macromolecular Science**, 2007.

ALHIJJAJ, Muqdad; BELTON, Peter; QI, Sheng. An investigation into the use of polymer blends to improve the printability of and regulate drug release from pharmaceutical solid dispersions prepared via fused deposition modeling (FDM) 3D printing. **European Journal of Pharmaceutics and Biopharmaceutics**, v. 108, p. 111-125, 2016.

BOELTER, Ruben; CHAGAS, Ana Maria; CUNHA, Carlos Mario. Ação Nefrotóxica após o uso parenteral de Neomicina em cães. **Revista do Centro de Ciências Rurais UFSM**. vol. 8 n.1, 1978.

CANDIDO, Juliana Dumard Carracena. **Síntese e caracterização de hidrogéis com micropartículas de alginato carregados com neomicina e própolis**. Rural Federal University of Rio de Janeiro Master's Thesis in Chemical Engineering. Seropédica. 2019.

DE ALMEIDA, A. M. G. **Estudo da possibilidade de utilização do polímero acrilonitrilo-butadieno-estireno processado via impressão 3d para produção de embalagens retornáveis de fluxos logísticos para a indústria automotiva**. Undergraduate Thesis – Material Engineering Degree. Federal Center for Technologic Education of Minas. Belo Horizonte. 2016.

DE KNEGT, Fernanda Triani Gomes. **Aspectos epidemiológicos e microbiológicos da espécie Staphylococcus pseudintermedius nas piodermites caninas: uma revisão da literatura**. Graduate Thesis – Microbiological Diagnosis and Control. Federal University of Minas Gerais. Belo Horizonte. 2018.

DEVRIESE, AN S.; BOELAERT, Johan R.; VANDERCASTEELE, Stefaan J. Staphylococcus aureus Infections in Hemodialysis: What a Nephrologist Should Know. **Clinical Journal of the American Society of Nephrology**. Ed. 8. Vol. 4, 2019.

EL-SAY, K. M.; EL-SAWY, H. S. **Polymeric nanoparticles: a promising platform for drug delivery. Methods in molecular biology**, v. 528, p.16675-16691, 2017.

HIRAYAMA, D. **Reciclagem do copolímero acrilonitrila-butadieno-estireno e do poliestireno de alto impacto oriundos de rejeitos de equipamentos elétricos e eletrônicos na forma de blendas poliméricas**. 2015. 213 p. Master's Thesis in Engineering. Federal University of São Paulo. Lorena. 2015.

LUNA, Carlos B.B.; SIQUEIRA, Danilo D.; ARAÚJO, Edcleide M.; WELLEN, Renate M. R.; MÉLO, Tomás Jeferson Alves de. Approaches to the acrylonitrile-butadiene-styrene functionalization through maleic anhydride and dicumyl

peroxide. **Journal of Vinyl & Additive Technology**, p.4 2020.

MAGLEBY, Reed; BEMIS, David A.; KIM, David; KANIA, Stephen; JENKINS, Stephen G.; WESTBLADE, Lars F.; CARROLL, Karen C.; CASTANHEIRA, Mariana. First reported human isolation of Staphylococcus delphine. **Diagnostic Microbiology and Infectious Disease**, v. 94, n. 3, p. 274-276, 2019.

MCVEY, D. Scott; KENNEDY, Melissa; CHENGAPPA, M. M. (Ed.). Veterinary microbiology. **John Wiley & Sons**, p. 184-193, 2013.

MELO, Ubiratan Pereira; FERREIRA, Cintia; FEIJÓ, Francisco Marlon Carneiro; SANTOS, Caio Sérgio. Pleuropneumonia séptica em potro**. Brazilian Journal of Animal and Environmental Research**, v. 4, n. 3, p. 3818-3831, 2021.

MIR, Mariam; ANSARI, Umar; ALI, Murtaza Najabat. Macro-scale model study of a tunable drug dispensation mechanism for controlled drug delivery in potential wound-healing applications. **Journal of applied biomaterials & functional materials**, v. 15, p. 63-69, 2017.

NARCISO, A.; FONSECA, Filipa; CERQUEIRA, Sofia Arriaga; DUARTE, Ainda. Susceptibilidade aos antibióticos de bactérias responsáveis por cistites não complicadas: estudo comparativo dos isolados de 2008 e 2010. **Acta Urológica**, v. 1, n. Março, p. 16–21, 2011.

NEHER, Gudrun.; GAFUR, Md. Abdul.; AL-MANSUR, Muhammad Abdullah.; BHUIYAN, Md. Mahbubur Rahman.; QADIR, Md. Rakibul.; AHMED, Farid. Investigation of the Surface Morphology and Structural Characterization of Palm Fiber Reinforced Acrylonitrile Butadiene Styrene (PF-ABS) Composites. **Journal Material Sciences and Applications**, 2014.

OLIVEIRA, R. A. G.; LIMA, E. O.; VIEIRA, W. L.; FREIRE, K. R L.; TRAJANO, V. N.; LIMA, I. O.; SOUZA, E. L.; TOLEDO, M. S.; SILVA-FILHO, R. N. Estudo da 92 interferência de óleos essenciais sobre a atividade de alguns antibióticos usados na clínica. **Revista Brasileira de Farmacognosia**, v.16(1): 77-82, 2006.

REBITSKI, Ediana P.; ALCÂNTARA, Ana C. S; DARDER, Margarita; CANSIAN, Rogério L.; GÓMEZ-HORTIGÜELA, Luis; PERGHER, Sibele B. C. **Functional Carboxymethylcellulose/Zein Bionanocomposite Films Based on Neomycin Supported on Sepiolite or Montmorillonite Clays**. ACS Omega, 2018

RESTANI, R. B.; CORREIA, V. G.; BONIFÁCIO, V. D. B.; AGUIARRICARDO, A. Development of functional mesoporous microparticles for controlled drug delivery. **The Journal of Supercritical Fluids**, v. 55, p.333-339, 2010.

SAKS, S. R.; GARDNER, L. B. **The pharmacoeconomic value of controlled-release dosage forms. Journal of Controlled Release**, v. 48, p.237-242, 1997.
SCHEIDT, D. T. **Eletrofiação da quitosana e sua aplicação como curativo para feridas**. 2018. 115 f. Master's Thesis in Chemistry. State University of Western Paraná. Toledo. 2018.

SHISHAVAN, Sajjad Mamaghani; AZDAST, Taher; AHMADI, Samrand Rash. Investigation of the effect of nanoclay and processing parameters on the tensile strength and hardness of injection molded Acrylonitrile Butadiene Styrene–organoclay nanocomposites. **Journal Materials & Design**, v. 58, p. 527-534, 2014.

SIMIELLI, Edson Roberto. Principais características das blendas poliméricas fabricadas no Brasil. **Polímeros: Ciência e tecnologia**, v. 3, n. 1, p. 45-49, 1993

SINGH, Mahima; JONNALAGADDA, Sriramakamal. Design and characterization of 3D printed, neomycin-eluting poly-L-lactide mats for wound-healing applications. **Journal of Materials Science: Materials in Medicine**, v.32, n. 44, 2021.

SPINOSA, Helenice de Souza; GÓRNIAK, Silvana Lima; BERNARDI, Maria Martha. **Farmacologia aplicada à medicina veterinária**. [S.l: s.n.], 2017.

SWATHI, Vottikuti; VIDYAVATHI, Maravajhala; PRASAD, TNVKV; KUMAR, R.V. Suresh. Design, Characterization and Evaluation of Metallic Nano Biocomposites of Neomycin. **Journal of Applied Solution Chemistry and Modeling**, p. 136-144, 2013.

TALÉNS - VISCONTI, R.; GARRIGUES, T. M.; CANTÓN, E. Mecanismos de resistencia bacteriana a las quinolonas. **Revista Espanola de Quimioterapia**, v. 15, nº1, 2002.